Original Article: The immobilized SbF_x species on copper or nickel ferrite as magnetic nanocatalysts for fast and convenient reduction and reductive acetylation of nitroarenes as well as acetylation of arylamines

Behzad Zeynizadeh* | **Marzieh Khanmirzaee** | **Maedeh Rabiei**

Faculty of Chemistry, Urmia University, Urmia 5756151818, Iran

Use your device to scan and read the article online

Citation B. Zeynizadeh*, M. Khanmirzaee, M. Rabiei. **The immobilized SbF_x species on copper or nickel ferrite as magnetic nanocatalysts for fast and convenient reduction and reductive acetylation of nitroarenes as well as acetylation of arylamines**. *J. Appl. Organomet. Chem.*, **2021**, *1*(4), 174-196.

https://doi.org/10.22034/jaoc.2021.303399.1035.

CC BY

Article info:
Received: September 06, 2021
Accepted: December 12, 2021
Available Online:
ID: JAOC-2109-1035
Checked for Plagiarism: Yes
Peer Reviewers Approved by:
Dr. Fatemeh Mohajer
Editor who Approved Publication:
Professor Dr. AbdelkaderZarrouk

Keywords:
Arylamines, $CuFe_2O_4@SbF_x$, $NiFe_2O_4@SbF_x$, Nitroarenes, Reduction, Reductive acetylation

ABSTRACT

In this study, magnetic nanoparticles (MNPs) of the immobilized SbF_x species on copper or nickel ferrite as $CuFe_2O_4@SbF_x$ and $NiFe_2O_4@SbF_x$ were synthesized. Fourier-transform infrared spectroscopy (FTIR), scanning electron microscopy (SEM), energy-dispersive X-ray spectroscopy (EDX), X-ray diffraction (XRD), vibrating sample magnetometer (VSM), Brunauer-Emmett-Teller (BET) analysis, and inductively coupled plasma optical emission spectroscopy (ICP-OES) were employed to characterize the prepared nanocatalysts. The catalytic activity of the nanomaterials was more studied towards reduction and reductive acetylation of structurally diverse aromatic nitro compounds as well as acetylation of arylamines. Among the examined nanocatalyst systems, $CuFe_2O_4@SbF_x$ was used for reduction and reductive acetylation of aromatic nitro compounds, whereas, $NiFe_2O_4@SbF_x$ showed activity towards acetylation of arylamines. All reactions were carried out successfully in H_2O as a green solvent under reflux conditions. After completion of the reactions, the examined nanocatalysts were easily removed from the reactions mixture by an external magnetic field. Their reusability was also examined for 5 consecutive cycles without the significant loss of the catalytic activity.

Introduction

Amines are extensively present in plants and animals. Biogenic amines such as histamine have many vital uses in the human body [1]. In this context, arylamines are the forerunner materials in the industry to produce colors, pesticides, herbicides, and photochromic compounds [2]. So, the reduction of aromatic nitro compounds is one of the straightforward methods for preparing arylamines [3].

*Corresponding Author: Behzad Zeynizadeh (bzeynizadeh@gmail.com)

Over the past decades, $NaBH_4$ has been frequently used as a mild reducing agent in modern organic synthesis. It is also known that the lonely $NaBH_4$ cannot reduce nitro compounds under ordinary conditions, however, the reducing capability of this reagent in the presence of various additives such as metal halides [4, 5] was exceptionally promoted towards reduction of nitro functionality.

The literature review shows that execution of the reactions under green conditions needs catalyst systems with high reactivity, extreme surface area, and good separable property. These characteristics could be easily and efficiently achieved by nanotechnology [6]. In this context, the importance and applications of nanostructured materials have been well documented in all aspects of science and technology [7-12].

Among the numerous nanomaterial systems, the use of magnetic nanoparticles has attracted a great deal of attention because of biocompatibility, ease of surface modification, inherent magnetic property, ease of separation by an external magnetic field, and high potentiality to use in various fields of industry [13]. In this area, the application of ferrites in various catalytic reactions shows the great conveniences of magnetic materials [14-21]. It is also well known that the good physical and chemical properties of spinel ferrites are due to the distribution of metal cations with different oxidation states between octahedral and tetrahedral sites [22-24]. In this area, copper and nickel spinel ferrites are the widely used magnetic metal oxides because of nontoxicity, biocompati-bility, high thermal stability up to 900 °C without losing the magnetic property, and effective catalytic activity in various processes [25-34]. These great characteristics make them susceptible to consider as the best candidates to modify their surfaces with different metal species for the promotion of various organic transformations.

Aligned with the outlined strategies, herein, the present work reveals the immobilization of SbF_x on the surface of $CuFe_2O_4$ and $NiFe_2O_4$ MNPs to afford the magnetic nanoparticles of $CuFe_2O_4$@SbF_x and $NiFe_2O_4$@SbF_x. These nanocomposites were easily separated from the reaction mixture by an external magnetic field. After washing with EtOAc, they could be recycled and reused for 5 consecutive cycles without the significant loss of the catalytic activity. The obtained results exhibited that reduction and reductive acetylation of aromatic nitro compounds were carried out efficiently with $CuFe_2O_4$@SbF_x MNPs. As well, due to the importance of the protection of amines as one of the widely used strategies in the multistep synthesis of organic compounds [35-44], using $NiFe_2O_4$@SbF_x MNPs towards *N*-acetylation of arylamines was also examined successfully (Figures 1 and 2).

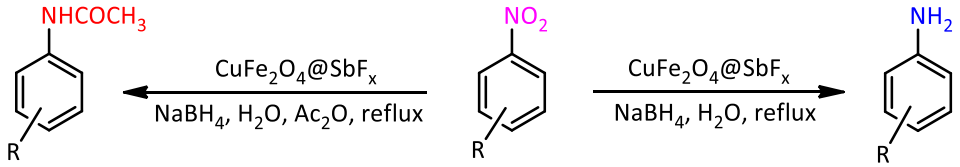

Figure 1. Reduction and reductive acetylation of nitroarenes by $NaBH_4$/$CuFe_2O_4$@SbF_X system

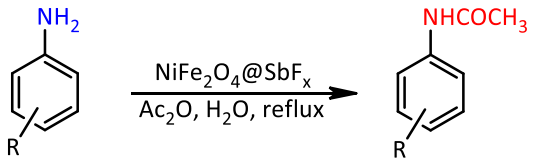

Figure 2. *N*-Acetylation of arylamines with $NiFe_2O_4$@SbF_X/Ac_2O system

Experimental

All reagents and materials were purchased from chemical sources and they were used without further purification. A Thermo Nicolet Nexus 670 spectrometer was used to record Fourier transform infrared spectra of the materials. X-ray diffraction (XRD) measurements were fulfilled on X'Pert Pro Panalytical diffractometer at 40 kV/30 mA with a Cu Kα radiation (λ=1.5418 A°). Signal data were recorded in 2θ = 10°–80° with a step interval of 0.05°. A FESEM-TESCAN MIRA3 apparatus was utilized to determine the morphology and size distribution of particles by scanning electron microscopy (SEM) method. This apparatus was also used to reveal the chemical composition of the nanocatalysts through the energy-dispersive X-ray spectroscopy (EDX) technique. The BET (Brunauer–Emmett–Teller) surface area, pore-volume, and pore diameter of the samples were measured using Belsorp-Max, Japan. Vibrating sample magnetometer (VSM, Meghnatis Daghigh Kavir Co., Iran) analysis under magnetic field up to 20 kOe was applied to determine the magnetic property of the samples. Ni, Cu, Fe, and Sb contents of the nanocatalysts were determined by inductively coupled plasma optical emission spectroscopy (ICP-OES) on Optima 7300D spectrophotometer. Ultrasonic irradiation was carried out in SOLTEC SONICA 2400MH S3 (305 W). ^{1}H and ^{13}C NMR spectra were recorded on 300 MHz Bruker spectrometer. Thin-layer chromatography (TLC) was utilized to determine the purity of products and to monitor the progress of reactions using SILG/UV 254 aluminum sheets

Synthesis of $CuFe_2O_4$ and $NiFe_2O_4$ MNPs

The magnetic nanoparticles of $CuFe_2O_4$ and $NiFe_2O_4$ were synthesized based on the reported procedure [29]. A mixture of $Cu(OAc)_2{\cdot}H_2O$ or $Ni(OAc)_2{\cdot}4H_2O$ (1 mmol), $Fe(NO_3)_3{\cdot}9H_2O$ (2 mmol), NaOH (8 mmol), and NaCl (2 mmol) was grinded at room temperature for 50 min. During of the reaction, the color of the mixture was changed from blue to brown and then to black. The reaction was accompanied by the release of heat. Next, the mixture was washed with deionized water to remove the residue of sodium chloride and then filtered. The obtained solid materials were dried at 80 °C for 2 h and then grinded for 10 min. Calcination of the grinded materials at 700 °C for 5 h afforded the black nanoparticles of $CuFe_2O_4$ or $NiFe_2O_4$.

Synthesis of $CuFe_2O_4$@SbF_x and $NiFe_2O_4$@SbF_x MNPs

A mixture of $CuFe_2O_4$ or $NiFe_2O_4$ MNPs (1 g) in deionized H_2O (20 mL) was irradiated by ultrasound for 30 min. Then, a solution of SbF_3 (0.25 g) in deionized H_2O (5 mL) was added and the resulting mixture was sonicated for 30 min followed by stirring for 12 h under reflux conditions. Separation of the nanoparticles by magnetic decantation and then washing with deionized H_2O afforded $CuFe_2O_4$@SbF_x or $NiFe_2O_4$@SbF_x MNPs for further drying under air atmosphere.

A typical procedure for reduction of nitrobenzene with NaBH4/CuFe2O4@SbFx MNPs

In a round bottom flask (10 mL) equipped with a magnetic stirrer, a mixture of nitrobenzene (0.123 g, 1 mmol) in deionized H_2O (2 mL) was prepared. $CuFe_2O_4$@SbF_x MNPs (50 mg) was added and the resulting mixture was stirred for 2 min. After that, $NaBH_4$ (0.076 g, 2 mmol) was added and the mixture stirring was continued for 10 min under reflux conditions. Progress of the reaction was monitored by TLC (eluent: *n*-hexane/EtOAc: 10/2). After completion of the reaction, H_2O (5 mL) was added and the mixture was stirred for 2 min at room temperature. Nanoparticles of $CuFe_2O_4$@SbF_x were separated by magnetic decantation and the product was extracted using EtOAc (3 × 5 mL). The combined extracts were dried over anhydrous Na_2SO_4. Evaporation of the solvent under reduced pressure afforded the pure liquid aniline in 95% yield (0.088 g, Table 2, entry 1).

A typical procedure for reductive acetylation of nitrobenzene with $NaBH_4/CuFe_2O_4@SbF_x/Ac_2O$ system

In a round bottom flask (10 mL) equipped with a magnetic stirrer, a mixture of nitrobenzene (0.123 g, 1 mmol) in deionized H_2O (2 mL) was prepared. $CuFe_2O_4@SbF_x$ MNPs (50 mg) was added and the resulting mixture was stirred for 2 min. After that, $NaBH_4$ (0.076 g, 2 mmol) was added and the mixture stirring was continued for 10 min under reflux conditions. Progress of the reaction was monitored by TLC (eluent: *n*-hexane/EtOAc: 10/2). When the reduction of nitrobenzene was completed, Ac_2O (0.204 g, 2 mmol) was then added and the resulting mixture was stirred for 1 min. Progress of the *N*-acetylation of aniline was monitored by TLC. Next, H_2O (5 mL) was added and the mixture was stirred for 1 min at room temperature. Nanoparticles of $CuFe_2O_4@SbF_x$ were separated by magnetic decantation and the product was extracted using EtOAc (3 × 5 mL). The combined extracts were dried over anhydrous Na_2SO_4. Evaporation of the solvent under reduced pressure afforded the pure white crystals of acetanilide in 95% yield (0.128 g, Table 3, entry 1).

A typical procedure for N-acetylation of aniline catalyzed by $NiFe_2O_4@SbF_x/Ac_2O$ system

In a round bottom flask (10 mL) equipped with a magnetic stirrer, a mixture of aniline (0.093 g, 1 mmol) in deionized H_2O (2 mL) was prepared. $NiFe_2O_4@SbF_x$ MNPs (30 mg) was added and the resulting mixture was stirred for 2 min. After that, Ac_2O (0.204 g, 2 mmol) was added and the mixture stirring was continued for 1 min under reflux conditions. Progress of the reaction was monitored by TLC (eluent: *n*-hexane/EtOAc: 10/2). After completion of the reaction, H_2O (5 mL) was added and the mixture was stirred for 2 min at room temperature. Nanoparticles of $NiFe_2O_4@SbF_x$ were separated by magnetic decantation and the product was extracted using EtOAc (3 × 5 mL). The combined extracts were dried over anhydrous Na_2SO_4. Evaporation of the solvent under reduced pressure afforded the pure white crystals of acetanilide in 90% yield (0.122 g, Table 5, entry 1).

Results and discussion

Synthesis and characterization of $CuFe_2O_4@SbFx$ and $NiFe_2O_4@SbFx$ MNPs

The magnetic nanoparticles of $CuFe_2O_4@SbF_x$ and $NiFe_2O_4@SbF_x$ were prepared in a two-step procedure: copper and nickel ferrite as a magnetic core was primarily synthesized by solid-state grinding of $Cu(OAc)_2{\cdot}H_2O$ or $Ni(OAc)_2{\cdot}4H_2O$, $Fe(NO_3)_3{\cdot}9H_2O$, NaOH and NaCl in a molar ratio of 1:2:8:2, respectively, at room temperature followed by calcination of the resulting product at 700 °C. Then the antomonyl species were immobilized on the surface of magnetic cores. In this context, a mixture of copper or nickel ferrite and SbF_3 in deionized H_2O was exposed to ultrasonic waves followed by refluxing for 12 h. The resulting nanoparticles were separated by an external magnetic field and washed several times with deionized water and then dried under an air atmosphere.

SEM analysis

To study the morphology and size distribution of $CuFe_2O_4$, $CuFe_2O_4@SbF_x$, $NiFe_2O_4$, and $NiFe_2O_4@SbF_x$ MNPs, scanning electron microscopy (SEM) analysis was carried out over the materials. The images for $CuFe_2O_4$ (Figure 3a) and $CuFe_2O_4@SbF_x$ (Figure 3b) show that the composite systems were constructed from roughly and granular particles with high porosity. As well, the particles are not aggregated and well distributed in the range of nanometer. The average particle size in $CuFe_2O_4$ and $CuFe_2O_4$ $@SbF_x$ MNPs is about 36-49 and 50-100 nm, respectively. In the case of $NiFe_2O_4$ (Figure 3c) and $NiFe_2O_4@SbF_x$ (Figure 3d) MNPs, however, an extent to the aggregation of particles is observed. In addition, the porosity of $NiFe_2O_4$ and $NiFe_2O_4@SbF_x$ in comparison to $CuFe_2O_4$ and $CuFe_2O_4@SbF_x$ was reduced. Nevertheless, the particles were distributed in nanometer range from 18-24 and 28-46 nm, respectively.

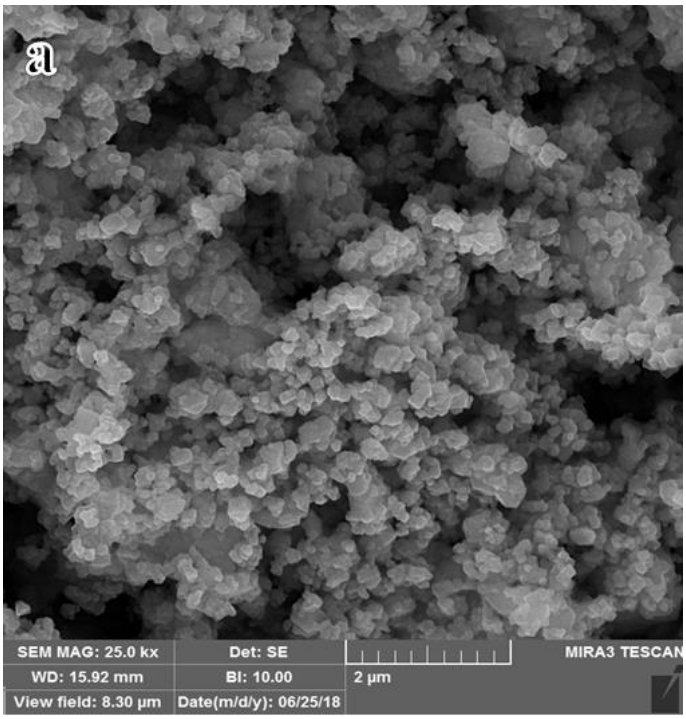
a
SEM MAG: 25.0 kx
Det: SE
MIRA3 TESCAN
WD: 15.92 mm
BI: 10.00
2 µm
View field: 8.30 µm
Date(m/d/y): 06/25/18

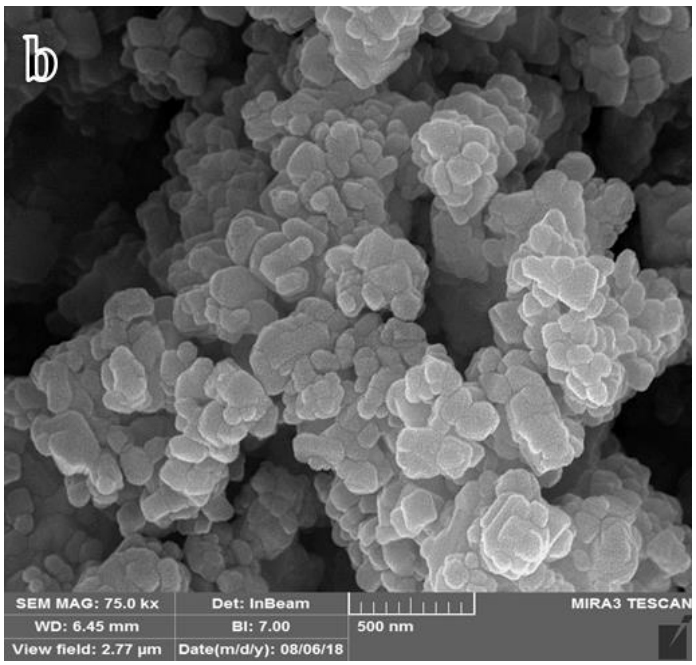
b
SEM MAG: 75.0 kx
Det: InBeam
MIRA3 TESCAN
WD: 6.45 mm
BI: 7.00
500 nm
View field: 2.77 µm
Date(m/d/y): 08/06/18

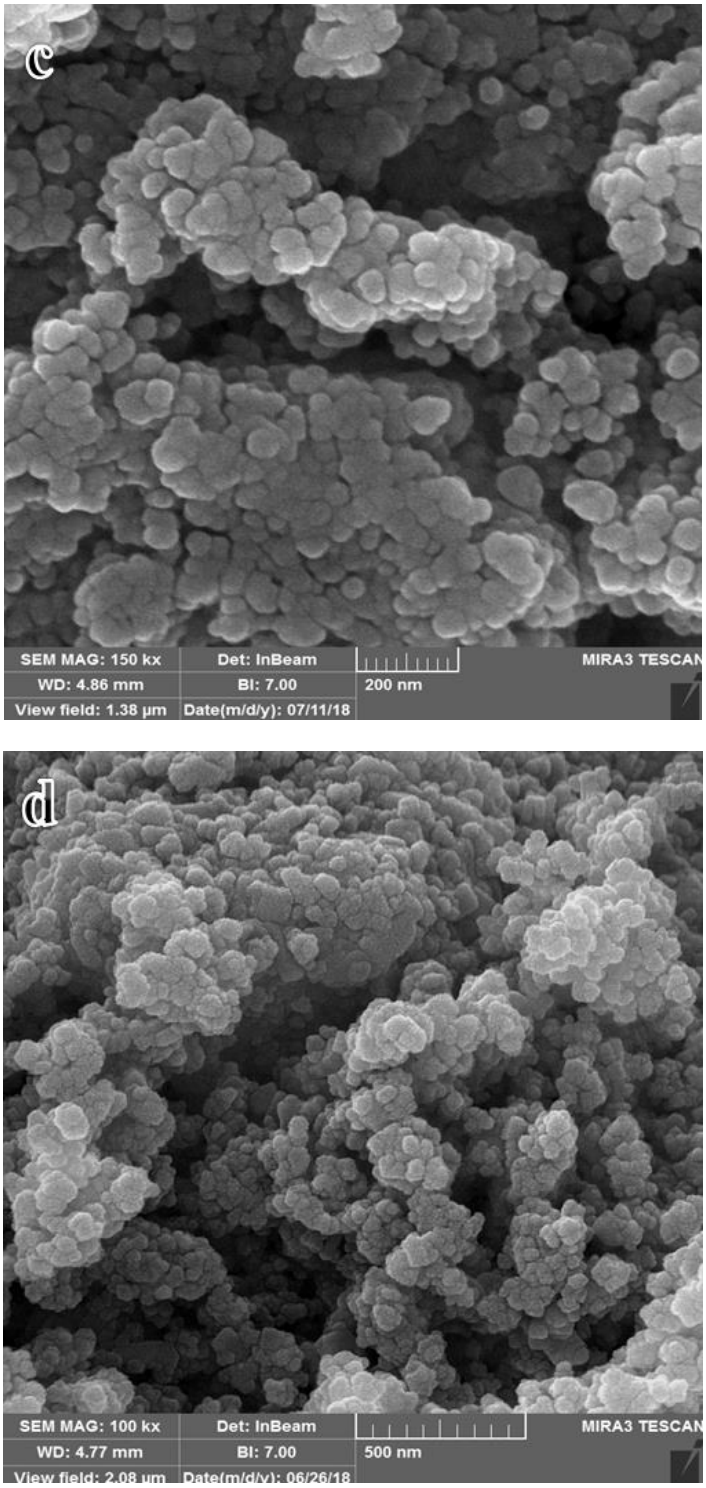

Figure 3. SEM images of **a** $CuFe_2O_4$, **b** $CuFe_2O_4@SbF_x$, **c** $NiFe_2O_4$ and **d** $NiFe_2O_4@SbF_x$ MNPs

EDX analysis

To determine the elemental composition of the examined nanocatalysts, energy dispersive X-ray spectroscopy (EDX) was taken place. Observation of the spectra for $CuFe_2O_4$, $CuFe_2O_4@SbF_x$, $NiFe_2O_4$, and $NiFe_2O_4@SbF_x$ MNPs reveals that all the magnetic materials

have the required elements in their composition systems (Figures 4a, b, c, and d).

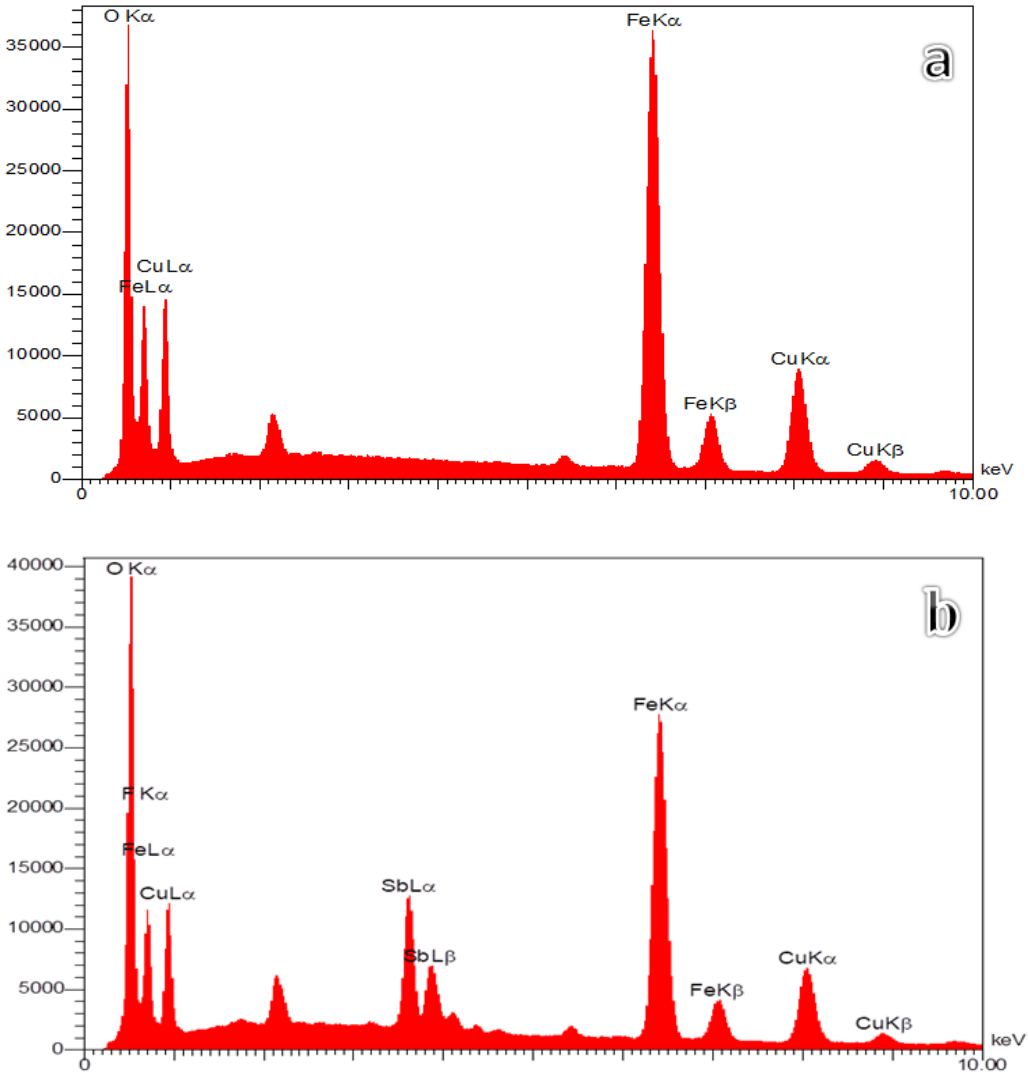

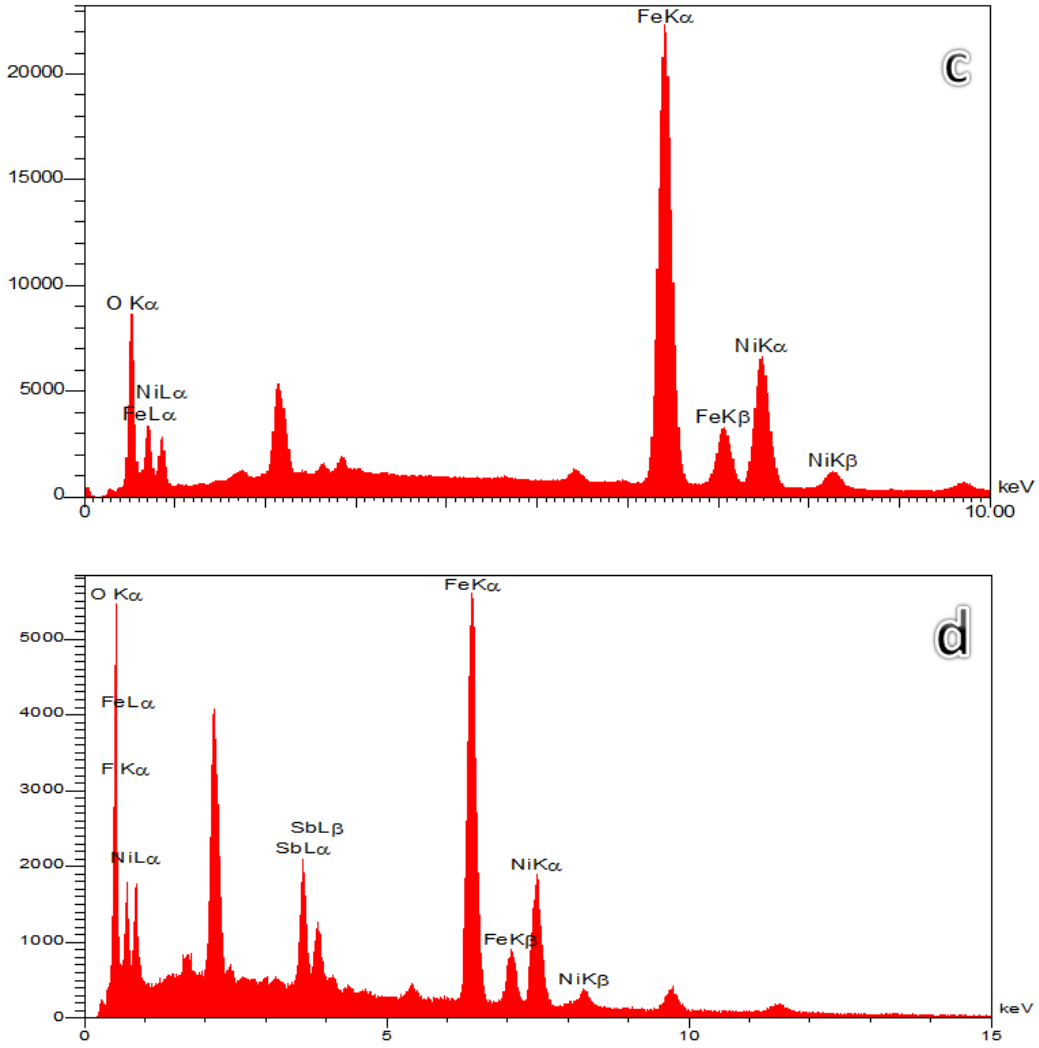

Figure 4. EDX analysis of **a** $CuFe_2O_4$, **b** $CuFe_2O_4$@SbF_X, **c** $NiFe_2O_4$ and **d** $NiFe_2O_4$@SbF_x MNPs

VSM analysis

Vibrating sample magnetometer (VSM) analysis was used to measure and compare the magnetic property of the synthesized $CuFe_2O_4$, $CuFe_2O_4$@SbF_x, $NiFe_2O_4$, and $NiFe_2O_4$ @SbF_x MNPs. In the magnetic field up to 20 kOe, the saturation magnetization (Ms) value for $CuFe_2O_4$ and $CuFe_2O_4$@SbF_x is 17.11 and 13.68 emu·g^{-1}, respectively (Figures 5a and b). As well, the Ms value for $NiFe_2O_4$ and $NiFe_2O_4$@SbF_x is 14.25 and 18.57 emu·g^{-1}, respectively (Figures 5c and d). The obtained results reveal that through the immobilization of SbF_x species on the surface of magnetic cores, the saturation magnetization value of $CuFe_2O_4$@SbF_x in comparison to $CuFe_2O_4$ was decreased, whereas, the amount for $NiFe_2O_4$ @SbF_x relative to $NiFe_2O_4$ was increased. The difference in saturation magnetization behavior of $CuFe_2O_4$@SbF_x and $NiFe_2O_4$@SbF_x MNPs via the immobilization of SbF_x species is not clear, however, the kind of interaction of antimony species with central transition metals (Cu or Ni) maybe play a role to affect the magnetic influence of the resulted nanoparticles.

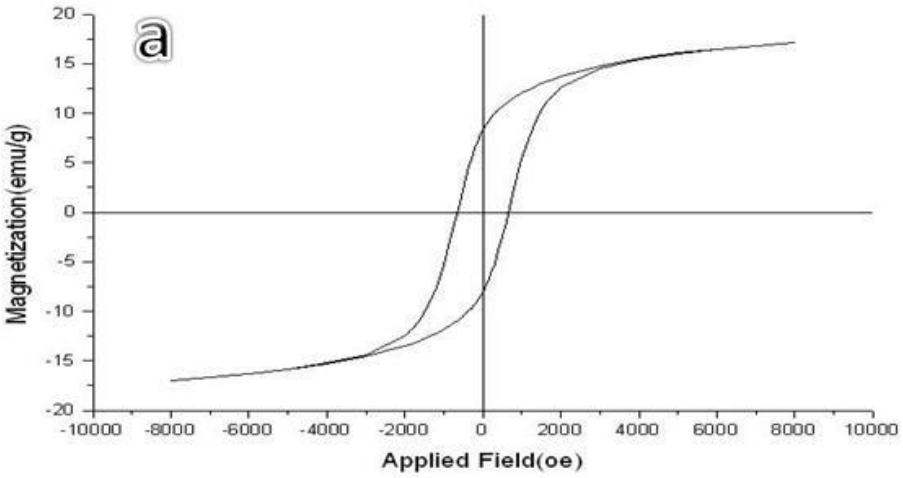
a
Magnetization(emu/g)
Applied Field(oe)
20
15
10
5
0
-5
-10
-15
-20
-10000
-8000
-6000
-4000
-2000
0
2000
4000
6000
8000
10000

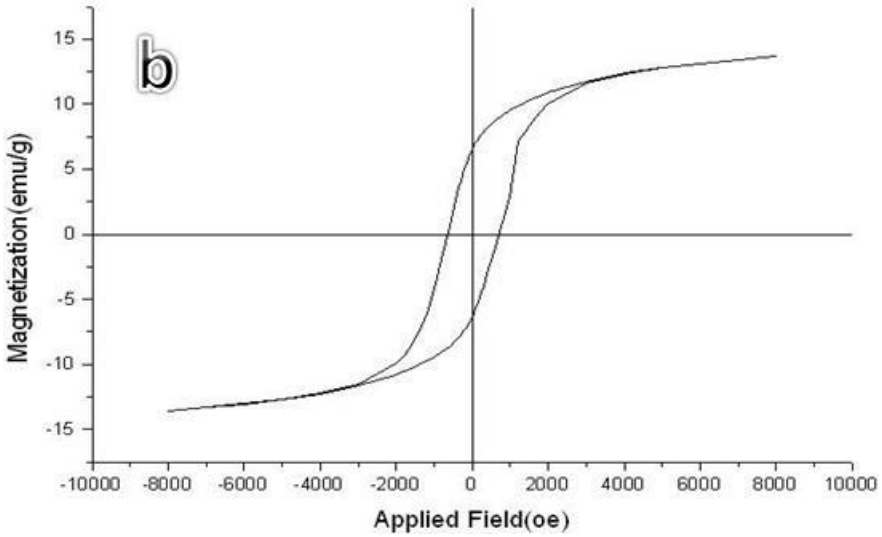
b
Magnetization(emu/g)
Applied Field(oe)
15
10
5
0
-5
-10
-15
-10000
-8000
-6000
-4000
-2000
0
2000
4000
6000
8000
10000

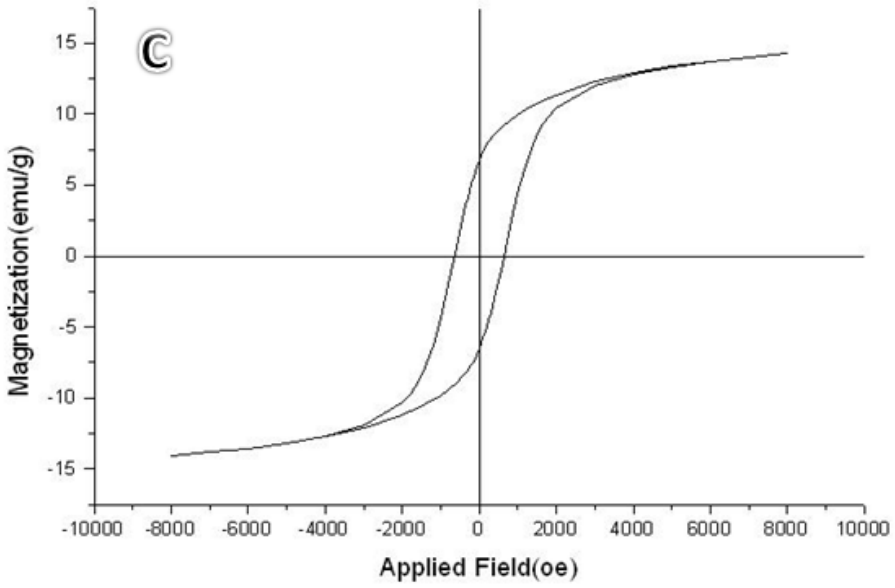
c
Magnetization(emu/g)
Applied Field(oe)
15
10
5
0
-5
-10
-15
-10000
-8000
-6000
-4000
-2000
0
2000
4000
6000
8000
10000

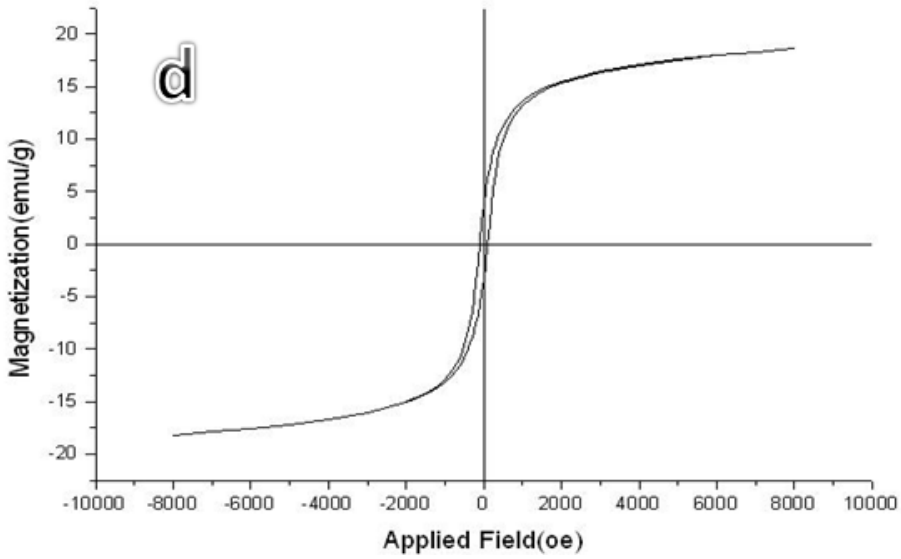

Figure 5. VSM analysis of **a** $CuFe_2O_4$, **b** $CuFe_2O_4$@SbF_x, **c** $NiFe_2O_4$ and **d** $NiFe_2O_4$@SbF_X MNPs

XRD analysis

Structural elucidation of $CuFe_2O_4$, $CuFe_2O_4$@SbF_x, $NiFe_2O_4$, and $NiFe_2O_4$@SbF_X MNPs was also carried out using X-ray diffraction (XRD) analysis. Primarily, the existence of individual sharp peaks in the depicted XRD patterns represents that all the examined nanomaterials have the extent of crystallinity character. The investigation for XRD pattern of $CuFe_2O_4$ (Figure 6a) and $CuFe_2O_4$@SbF_x MNPs (Figure 6b) shows the cubic spinel structure in the synthesized nanocatalysts. As well, the peak at $2\theta = 28°$ for $CuFe_2O_4$@SbF_x MNPs exactly refers to the exitance of Sb species [45]. In addition, the analysis for XRD pattern of $NiFe_2O_4$ (Figure 6c) and $NiFe_2O_4$@SbF_x (Figure 6d) shows the reverse spinel structure, and the presence of Sb species is also confirmed by a peak position at $2\theta = 28°$.

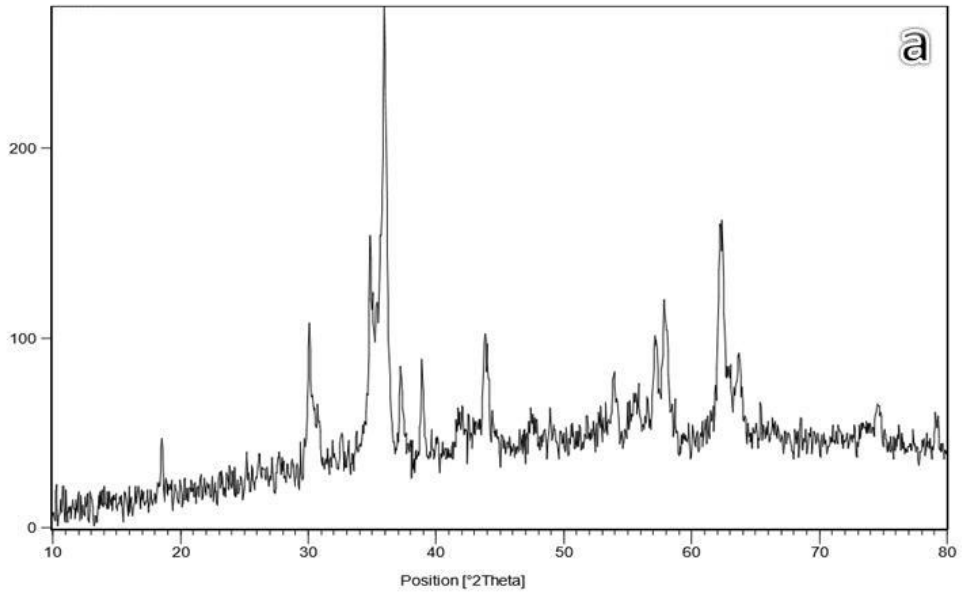

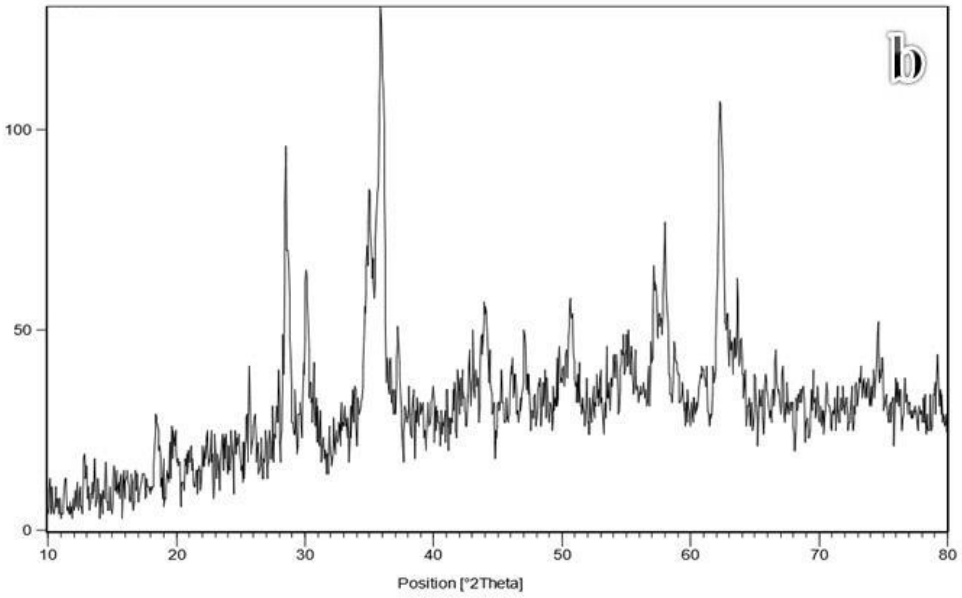
b
100
50
0
10
20
30
40
50
60
70
80
Position [°2Theta]

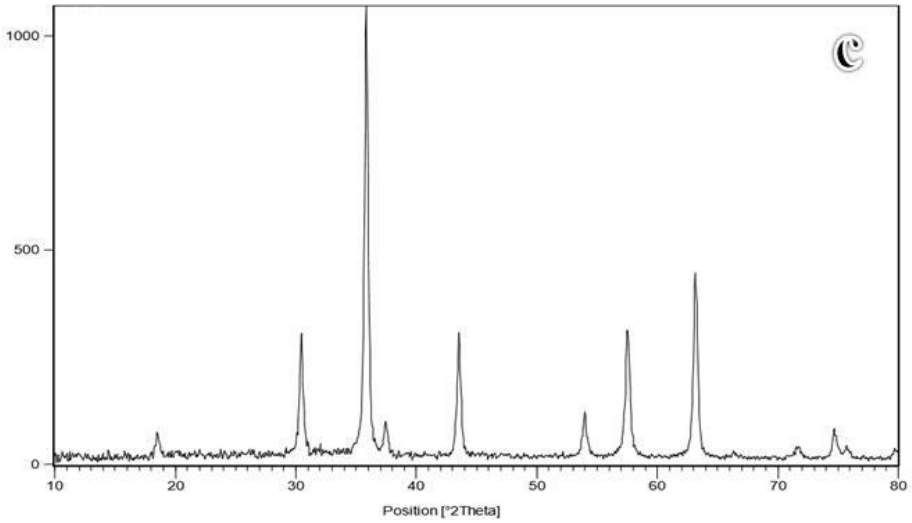
c
1000
500
0
10
20
30
40
50
60
70
80
Position [°2Theta]

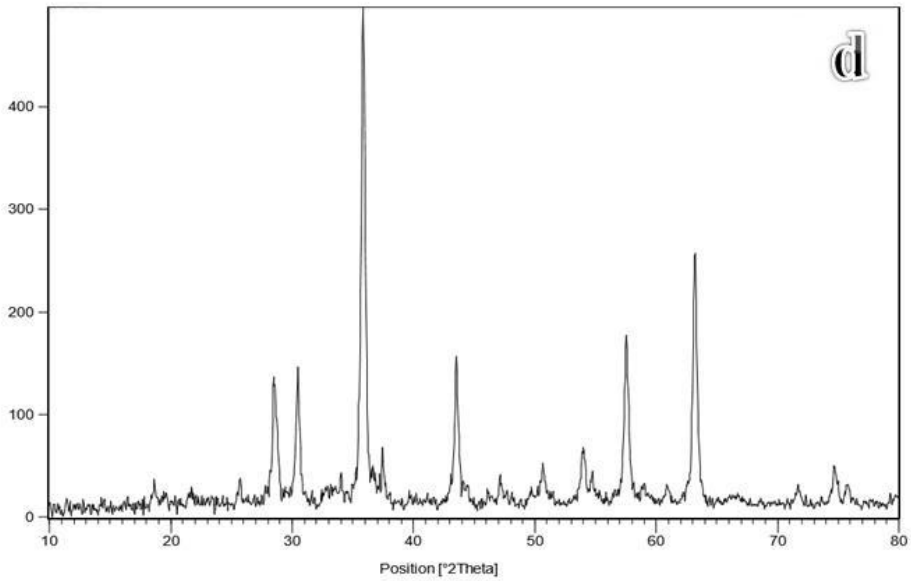

Figure 6. XRD analysis of **a** $CuFe_2O_4$, **b** $CuFe_2O_4$@SbF_x, **c** $NiFe_2O_4$, and **d** $NiFe_2O_4$@SbF_X

ICP analysis

Inductively coupled plasma optical emission spectrometry (ICP-OES) was used to exactly determine the amount of Cu, Ni, Fe, and Sb elements in the synthesized nanocatalysts. Based on the analyses, the weight percentage of Cu, Fe, and Sb in $CuFe_2O_4$@SbF_x was 21.27, 36.95, and 16.98%, respectively, and for Ni, Fe, and Sb in $NiFe_2O_4$@SbF_x was 10.94, 21.08, 12.04%.

BET analysis

In order to determine the specific surface area and pore volume of $CuFe_2O_4$@SbF_x (Figure 7a) and $NiFe_2O_4$@SbF_x (Figure 7b), the N_2 adsorption-desorption analysis (BET) was investigated. The results exhibit that the specific surface area of $CuFe_2O_4$@SbF_x and $NiFe_2O_4$@SbF_x MNPs is 6.12, 14.642 $m^2.g^{-1}$ and the pore volume is 0.07, 0.09 $cm^3.g^{-1}$, respectively.

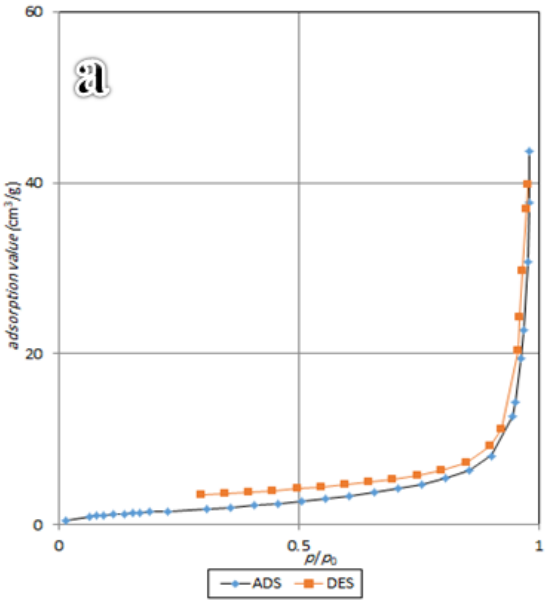

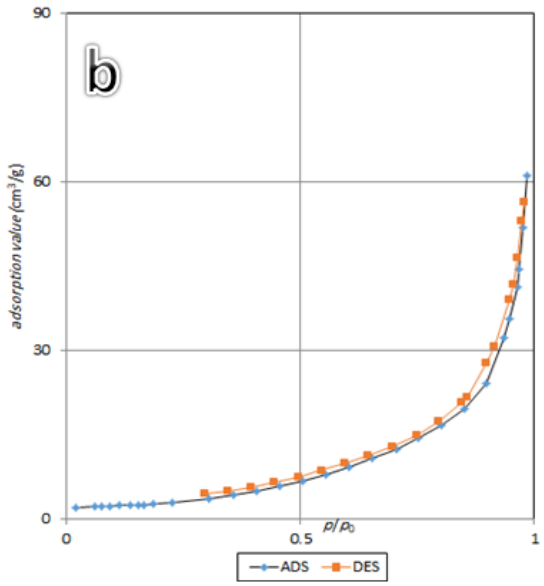

Figure 7. N_2 adsorption-desorption diagram of **a** $CuFe_2O_4@SbF_x$ and **b** $NiFe_2O_4@SbF_x$ MNPs

FTIR analysis

Structural elucidation of $CuFe_2O_4$, $CuFe_2O_4@SbF_x$, $NiFe_2O_4$, and $NiFe_2O_4@SbF_x$ MNPs was further studied by Fourier transform infrared spectroscopy. FTIR spectrum of $CuFe_2O_4$ (Figure 8), $NiFe_2O_4$ (Figure 9) has two high absorption peaks in the low energy area (1000 cm^{-1}) which is related to the vibration of Fe-O bond. The strong absorption peaks at 1633-2360 and 3426-3440 cm^{-1} are also attributed to O–H deforming and stretching vibrations of the adsorbed water, respectively. As well, the absorption peaks at 1249 and 1387 cm^{-1} are regarded to the presence of antimony species in $CuFe_2O_4@SbF_x$ and $NiFe_2O_4@SbF_x$ MNPs, respectively.

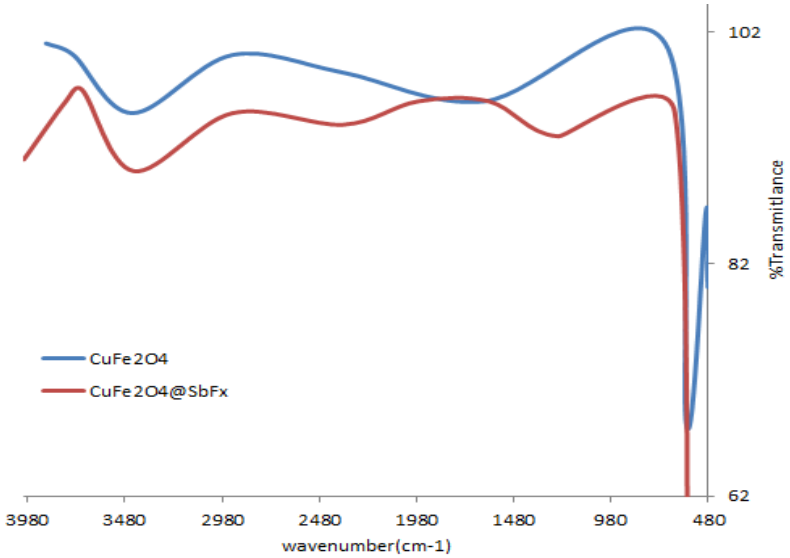

Figure 8. FTIR spectra of **a** $CuFe_2O_4$ and **b** $CuFe_2O_4@SbF_x$ MNPs

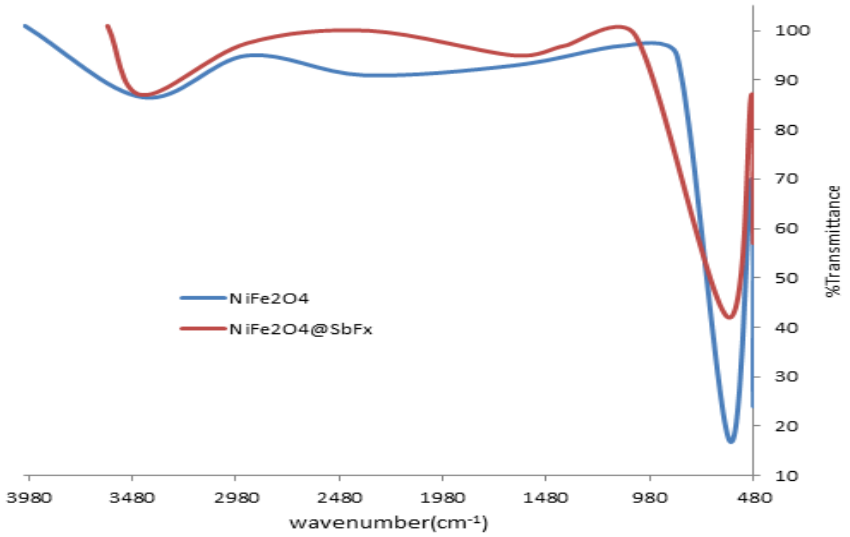

Figure 9. FTIR spectra of **a** $NiFe_2O_4$ and **b** $NiFe_2O_4$@SbF_x MNPs

The catalytic activity of $CuFe_2O_4$@SbF_x MNPs towards reduction of nitroarenes

After the synthesis and characterization of $CuFe_2O_4$@SbF_x MNPs and since of the wide-spread application of arylamines in organic synthesis, we were encouraged to investigate catalytic activity of the magnetic nanocatalyst towards reduction of nitroarenes. In this context, reduction of nitrobenzene with $NaBH_4$ in the presence of $CuFe_2O_4$@SbF_x MNPs was selected as a model reaction and therefore different reaction conditions such as the change of reaction solvent (H_2O, EtOH, and H_2O-EtOH), varying the amount of $NaBH_4$ and $CuFe_2O_4$@SbF_x MNPs, as well as the influence of temperature, were examined over the model reaction (Table 1). Based on the obtained results, reduction of nitrobenzene (1 mmol) with $NaBH_4$ (2 mmol) in the presence of $CuFe_2O_4$@SbF_x MNPs (50 mg) and in refluxing H_2O (2 mL) was selected as the optimum reaction conditions. Completion of the reaction was taken place in 10 min and the corresponding aniline was obtained in 95% yield (Table 1, entry 6)(Table 2, entry 1).

Table 1. Optimization experiments for reduction of nitrobenzene to aniline with $NaBH_4$/$CuFe_2O_4$@SbF_x MNPs systeam[a]

Entry	$NaBH_4$ (mmol)	$CuFe_2O_4$@SbF_x (mg)	Solvent	Condition	Time (min)	Conversion (%)
1	2	–	H_2O	reflux	120	trace
2	2	50	H_2O	r.t.	100	50
3	2	50	EtOH	reflux	5	100
4	3	50	H_2O:EtOH (1.5:0.5)	reflux	5	100
5	3	50	H_2O	reflux	5	100
6	2	50	H_2O	reflux	10	100
7	2	70	H_2O	reflux	5	100

[a]All reactions were carried out with 1 mmol of nitrobenzene in 2 mL solvent.

Next, the reducing capability of $NaBH_4$/$CuFe_2O_4$@SbF_x system was further studied towards the reduction of structurally different aromatic nitro compounds at the optimized reaction conditions. The results of this investigation are summarized in Table 2. The table shows that all aromatic nitro compounds using 2-3 mmol of $NaBH_4$ and 50 mg of $CuFe_2O_4$@SbF_x MNPs in refluxing H_2O (2 mL) were successfully reduced to the corresponding arylamines in 85-95% yields within 5-20 min. In addition, nitro compounds containing carbonyl functionality (aldehyde and ketone) were also successfully reduced without any selectivity among nitro and carbonyl groups and so the corresponding amino alcohols were obtained as the final products.

Table 2. Reduction of nitroarenes with $NaBH_4$/$CuFe_2O_4$@SbF_x system[a]

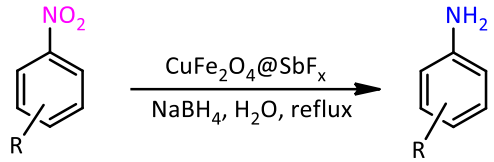

Entry	Substrate	Product	Molar Ratio[b]	Cat. (mg)	Time (min)	Yield (%)[c]
1	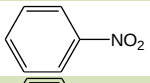	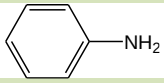	1:2	50	10	95
2	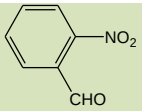	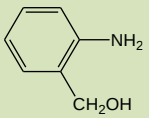	1:2	50	7	94
3	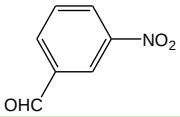	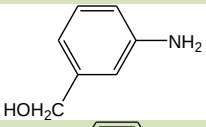	1:2	50	6	92
4		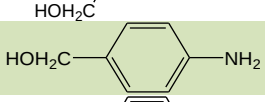	1:2	50	5	91
5	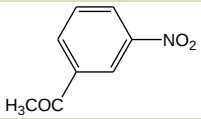	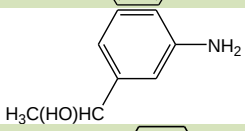	1:2	50	6	93
6	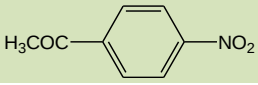	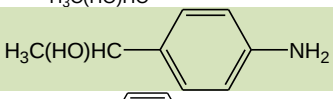	1:2	50	5	90
7[d]	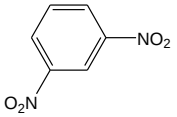	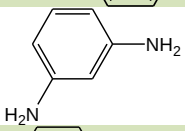	1:3	50	15	90
8	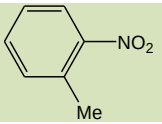	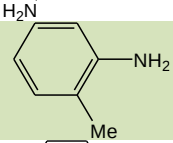	1:2	50	8	94
9	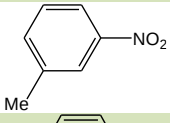	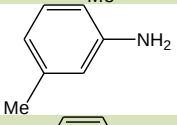	1:2	50	11	94
10			1:2	50	9	92

11	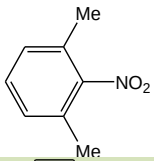	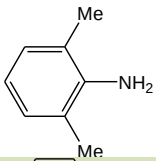	1:2	50	20	89
12	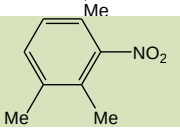	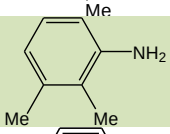	1:2	50	20	88
13	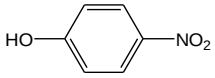	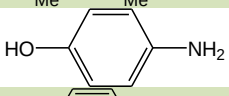	1:2	50	7	91
14	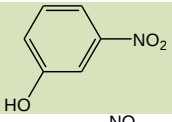	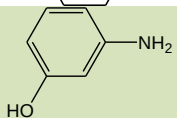	1:2	50	10	90
15[d]	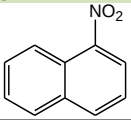	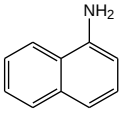	1:3	50	20	85

[a]All reactions were carried out in refluxing H_2O (2 mL). [b]Subs./$NaBH_4$. [c]Yields refer to isolated pure products. [d]$NaBH_4$ was added portion wisely.

The catalytic activity of $CuFe_2O_4$@SbF_x MNPs towards reductive acetylation of nitroarenes

Amides are useful intermediates in the production of many agricultural chemicals and industrial products. In this area, reductive acetylation of amines is the straightforward method for preparing of *N*-arylacetamides. This reaction could be taken place indirectly in a two-step procedure. Primarily, reduction of nitro compounds to the corresponding amines is carried out, and then the acetylation of isolated amines as a second step leads to the production of *N*-arylacetamides. The successful catalytic activity of $CuFe_2O_4$@SbF_x MNPs towards reduction of aromatic nitro compounds to arylamines with $NaBH_4$ encouraged us to study the capability of the examined nano catalyst towards reductive acetylation of nitroarenes without the isolation of the intermediate arylamines. In this context, reductive acetylation of nitrobenzene with $NaBH_4$/Ac_2O system in the presence of $CuFe_2O_4$@SbF_x MNPs was studied. In this context, when the reduction of nitrobenzene with $NaBH_4$/$CuFe_2O_4$@SbF_x system at the optimized reaction conditions was completed, Ac_2O (2 mmol) was added to the reaction mixture without the isolation of the produced aniline. Progress of the reaction was continued by the formation of acetanilide as a final product within 1 min. Therefore, reductive acetylation of nitrobenzene to acetanilide was taken place within 11 min (10 min for reduction of $PhNO_2$ to $PhNH_2$ and 1 min for the transformation of $PhNH_2$ to $PhNHCOCH_3$). Accordingly, reductive acetylation of structurally diverse nitroarenes was carried out by $NaBH_4$ (2 mmol)/$CuFe_2O_4$@SbF_x (50 mg)/Ac_2O (2 mmol) to afford the corresponding *N*-arylacetamides in high yields. The results of this investigation are summarized in Table 3. Investigation of the results exhibit that in the case of nitro compounds containing the functionality of carbonyl groups in which the reduction reaction produces amino alcohols as the intermediates, the further acetylation reaction was taken place only on the amino group and hydroxyl group was remained intact (Table 3, entries 7-9, 13 and 14). In the case of phenolic functionality in the presence of the amino group, however, the acetylation was carried out with the same reactivity on both functionalities (Table 3, entries 11 and 15).

Table 3. Reductive acetylation of aromatic nitro compounds with $NaBH_4/CuFe_2O_4@SbF_x/Ac_2O$ systeama

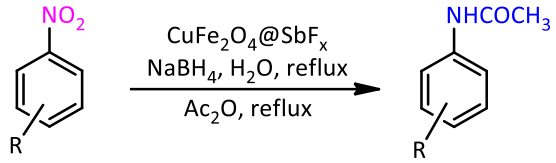

Entry	Substrate	Product	Molar Ratio[b]	Cat. (mg)	Time (min)	Yield (%)[c]
1	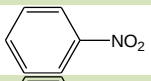	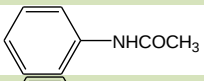	1:2:2	50	11	95
2	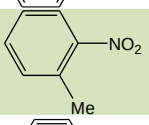	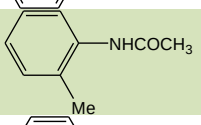	1:2:2	50	9	90
3	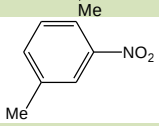	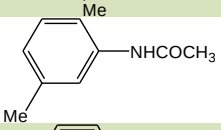	1:2:2	50	12	93
4	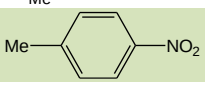	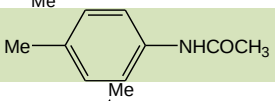	1:2:2	50	10	91
5	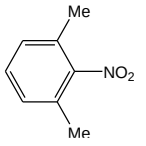	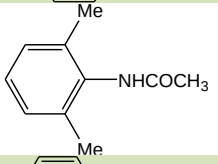	1:2:2	50	25	88
6	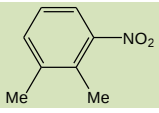	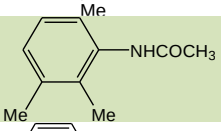	1:2:2	50	25	90
7	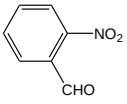	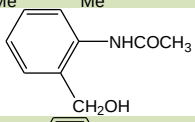	1:2:2	50	8	88
8	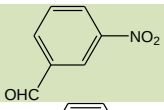	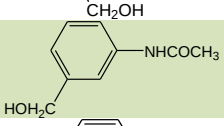	1:2:2	50	7	90
9	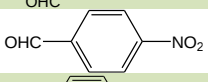	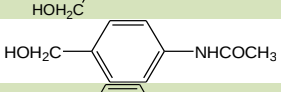	1:2:2	50	6	92
10[d]	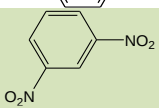	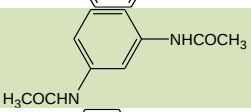	1:3:4	50	100	85
11	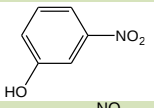	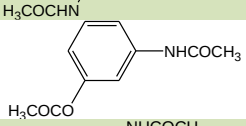	1:2:2	50	11	90
12[d]	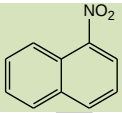	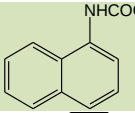	1:3:4	50	25	88
13	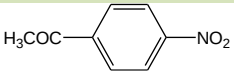	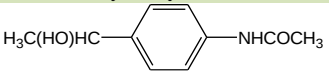	1:2:2	50	6	95

14	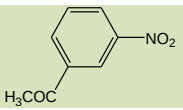	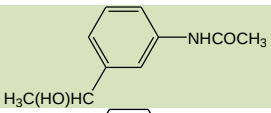	1:2:2	50	7	95
15	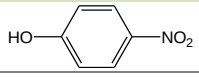	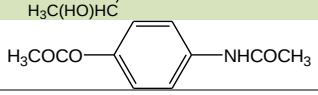	1:2:2	50	10	95

[a]All reactions were carried out in refluxing H_2O (2 mL). [b]Sub./$NaBH_4$/Ac_2O. [c]Yields refer to isolated pure products. [d]$NaBH_4$ was added portion wisely.

Although the exact mechanism of this synthetic protocol is not clear, however, $CuFe_2O_4$@SbF_x MNPs could be influenced by reduction of nitroarenes with $NaBH_4$ in two plausible pathways: in pathway i), transferring of hydride from sodium borohydride towards nitro group plays a key role. In pathway ii), $NaBH_4$ in aqueous media generates molecular H_2 and therefore its adsorption on the surface of nanocatalyst could be reduced nitro functionality (Figure 10).

Pathway i)

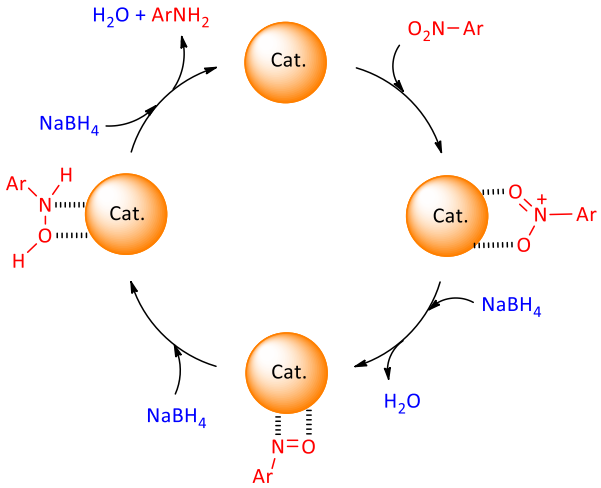

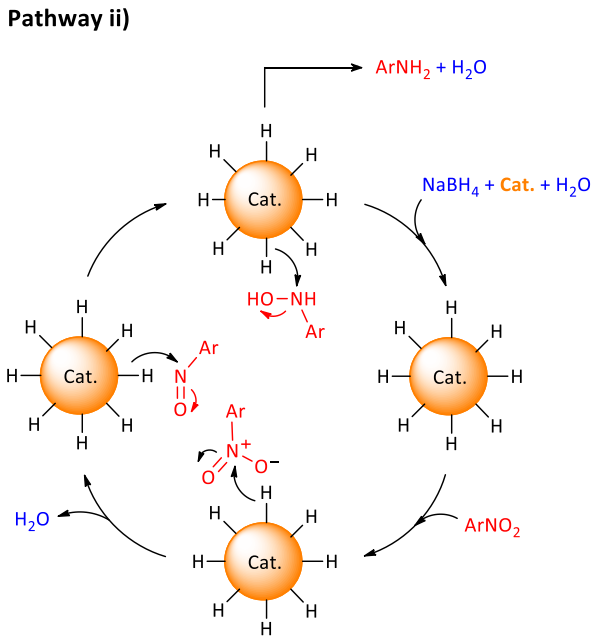

Figure 10. Plausible mechanisms for $NaBH_4$ reduction of nitroarenes catalyzed by $CuFe_2O_4@SbF_x$ MNPs

Acetylation of arylamines by $NiFe_2O_4@SbF_x$/Ac_2O system

Acetylation is a useful reaction for protecting amino groups in a multistep synthesis of complex organic molecules. Prompting by the successful catalytic activity of $CuFe_2O_4@SbF_x$ MNPs for reduction and reductive acetylation of aromatic nitro compounds, we decided to study the catalytic activity of $NiFe_2O_4@SbF_x$ MNPs for the acetylation of arylamines. In this context, aniline was selected as a model compound and therefore it was subjected to $NiFe_2O_4@SbF_x/Ac_2O$ system under different reaction conditions. Investigation of the results in Table 4 represents that 1 mmol of aniline in the presence of 2 mmol of Ac_2O and 30 mg of $NiFe_2O_4@SbF_x$ MNPs was success-fully acetylated within 1 min in refluxing H_2O (2 mL). As well, the corresponding acetanilide was obtained in 90% yield (Table 4, entry 5)(Table 5, entry 1).

Table 4. Optimization experiments for acetylation of aniline with $NiFe_2O_4@SbF_x/Ac_2O$ system[a]

Entry	$NiFe_2O_4@SbF_x$ (mg)	Ac_2O (mmol)	Solvent	Condition	Time (min)	Conversion (%)[b]
1	30	2	CH_2Cl_2	Reflux	120	70
2	30	2	THF	Reflux	120	60
3	30	2	CH_3CN	Reflux	120	40
4	30	2	H_2O:EtOH(1.5:0.5)	Reflux	10	100
5	30	2	H_2O	Reflux	1	100

[a]All reactions were carried out with 1 mmol aniline in 2 mL solvent. [c]onversion less than 100% was determined on the basis of the recovered aniline.

Continued by the success, acetylation of structurally different arylamines with $NiFe_2O_4@SbF_x/Ac_2O$ system at the optimized reaction conditions was carried out. The summarized results in Table 5 show that the arylamines using 2-4 mmol of Ac_2O and 30 mg of

$NiFe_2O_4@SbF_x$ MNPs in refluxing H_2O were easily acetylated to the corresponding *N*-arylacetamides within 1-18 min and 87-92% yield.

Table 5. Acetylation of aromatic amines with $NiFe_2O_4@SbF_x/Ac_2O$ system[a]

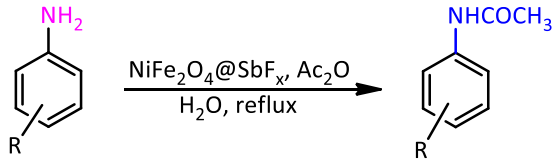

Entry	Substrate	Product	Molar Ratio[b]	Cat. (mg)	Time (min)	Yield (%)[c]
1	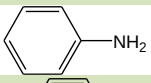	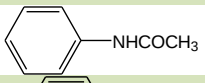	1:2	30	1	90
2	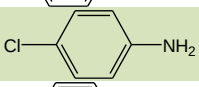	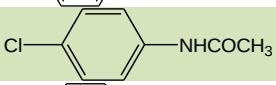	1:3	30	4	91
3	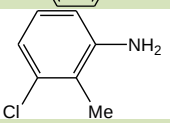	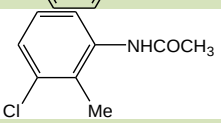	1:3	30	6	89
4	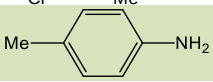	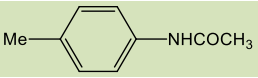	1:2	30	1	92
5	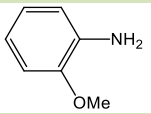	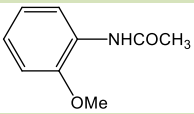	1:2	30	1	91
6	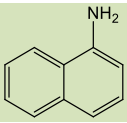	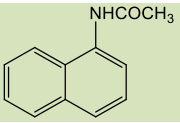	1:3	20	2	88
7		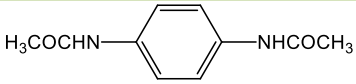	1:4	40	18	90
8	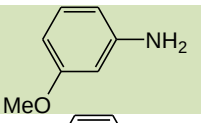	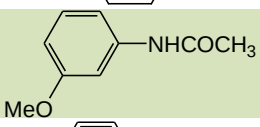	1:2	20	1	90
9	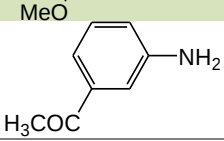	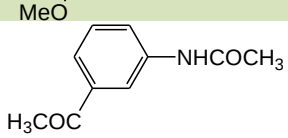	1:2	30	1	87

[a]All reactions were carried out in refluxing H_2O (2 mL). [b]Sub./Ac_2O. [c]Yields refer to isolated pure products.

Reusability

The economic and green aspects of the present protocols were also investigated by examining the reusability of $CuFe_2O_4@SbF_x$ and $NiFe_2O_4@SbF_x$ MNPs towards reduction and reductive acetylation of nitrobenzene as well as the acetylation of aniline. In this context, when the titled transformations were completed, the examined nanocatalysts were magnetically separated from the reaction mixture. The recycled nanocatalysts were washed with EtOAc and dried for reuse at the next runs. The given results in Figure 11 represent that the nanocatalysts can be reused for 5 consecutive cycles without the significant loss of the catalytic activity.

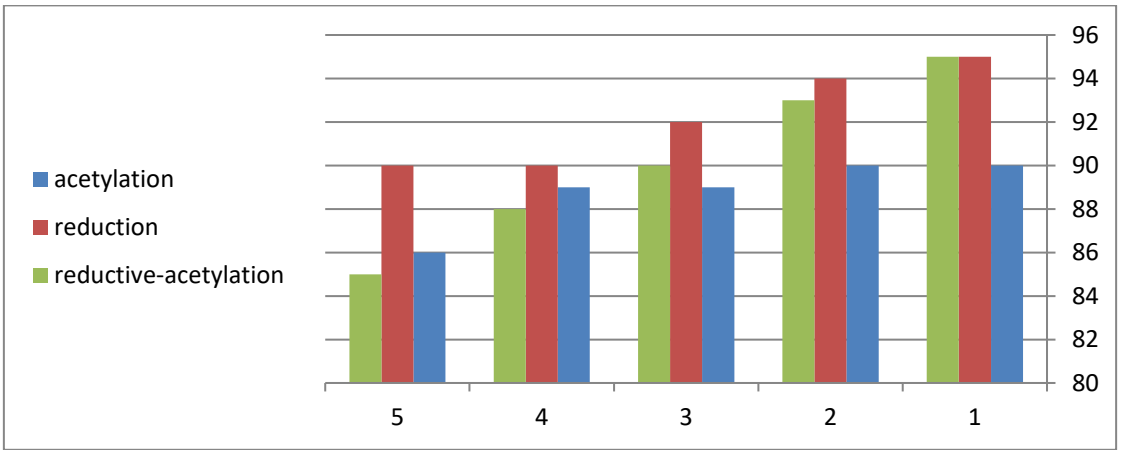

Figure 11. Reusability of $CuFe_2O_4$@SbF_x and $NiFe_2O_4$@SbF_x MNPs

Conclusion

In this paper, we have synthesized $CuFe_2O_4$ @SbF_x and $NiFe_2O_4$@SbF_x as novel magnetic nanocatalysts towards reduction and reductive acetylation of diverse aromatic nitro compounds as well as the *N*-acetylation of arylamines. Characterization of nanomaterials was carried out using FTIR, XRD, SEM, EDX, BET, and VSM analyses. $CuFe_2O_4$@SbF_x MNPs showed a significant catalytic activity towards reduction and reductive acetylation of nitroarenes, however, $NiFe_2O_4$@SbF_x MNPs showed activity for *N*-acetylation of aryl-amines. All reactions were carried out in H_2O as a green solvent under reflux conditions. The reusability of the nanocatalysts was examined for 5 consecutive cycles without the significant loss of the catalytic activity.

Acknowledgment

The authors gratefully appreciate the financial support of this work by the research council of Urmia University.

References

1. 1. B.T. Brink, C. Damink, H.M.L.J. Joosten, J.H.J. Huis in't Veld, *Int. J. Food Microbiol.*, **1990**, *11*, 73-84. **[Crossref], [Google Scholar], [Publisher]**
2. A.K. Shil, D. Sharma, N.R. Guha, P. Das, *Tetrahedron Lett.*, **2012**, *53*, 4858-4861. **[Crossref], [Google Scholar], [Publisher]**
3. R.S. Downing, P. J. Kunkeler, H.van Bekkum, Catal. Today., **1997**, 37, 121-136. **[Crossref], [Google Scholar], [Publisher]**
4. Gribble, G.W., 1997. Reductions in Organic Chemistry, By Milos Hudlicky (Virginia Polytechnic Institute and State University). American Chemical Society, Washington, DC. **1996**. **[Crossref], [Google Scholar], [Publisher]**
5. B. Zeynizadeh, T. Behyar, *J. Braz. Chem. Soc.*, **2005**, *16*, 1200-1209. **[Crossref], [Google Scholar], [Publisher]**
6. W. Liu, *China Particuology*, **2005**, *3*, 383-394. **[Crossref], [Google Scholar], [Publisher]**
7. I. Ali, O.M.L. Alharbi, Z.A. Alothman, A.Y. Badjah. *Photochem. Photobiol.*, **2018**, 94, 935-941. **[Crossref], [Google Scholar], [Publisher]**
8. I. Ali, H. Y. Aboul-Enein, *Crit. Rev. Anal. Chem.*, **2002**, *32*, 337-350. **[Crossref], [Google Scholar], [Publisher]**
9. I. Ali, O.M.L. Alharbi, A. Tkachev, E. Galunin, A. Burakov, V.A. Grachev, *Environ. Sci. Pollut. Res.*, **2018**, *25*, 7315-7329. **[Crossref], [Google Scholar], [Publisher]**
10. I. Ali, O.M.L. Alharbi, Z.A. Alothman, A. Alwarthan, *Colloids Surf. B: Biointerfaces*, **2018**, *171*, 606-613. **[Crossref], [Google Scholar], [Publisher]**

11. A. Jafari, B. Zeynizadeh, S. Darvishi, *J. Mol. Liq.*, **2018**, *253*, 119-126. [Crossref], [Google Scholar], [Publisher]
12. I. Ali, A.E. Burakov, A.V. Melezhik, A.V. Babkin, I.V. Burakova, E.A. Neskomornaya, E.V. Galunin, A.G. Tkachev, D.V. Kuznetsov, *Chem. Select*, **2019**, *4*, 12708-12718. [Crossref], [Google Scholar], [Publisher]
13. S.H. Joo, J.Y. Park, J.R. Renzas, D.R. Butcher, W. Huang, G. A. Somorjai, *Nano Lett.*, **2010**, *10*, 2709-2713. [Crossref], [Google Scholar], [Publisher]
14. G. Busca, E. Finocchio, V. Lorenzelli, M. Trombetta, S.A. Rossini, *J. Chem. Soc. Faraday Trans.*, **1996**, *92*, 4687-4693. [Crossref], [Google Scholar], [Publisher]
15. L. Dong, Z. Liu, Y. Hu, B. Xu, Y. Chen, *J. Chem. Soc. Faraday Trans.*, **1998**, *94*, 3033-3038. [Crossref], [Google Scholar], [Publisher]
16. N.J. Jebarathinam, M. Eswaramoorthy, V. Krishnasamy, *Bull. Chem. Soc. Jpn.*, **1994**, *67*, 3334-3338. [Crossref], [Google Scholar], [Publisher]
17. P. Lahiri, S.K. Sengupta, *J. Chem. Soc. Faraday Trans.*, **1995**, *91*, 3489-3494. [Crossref], [Google Scholar], [Publisher]
18. N.K. Singh, S.K. Tiwari, K.L. Anitha, R.N. Singh, *J. Chem. Soc. Faraday Trans.*, **1996**, *92*, 2397-2400. [Crossref], [Google Scholar], [Publisher]
19. J. Miki, M. Asanuma, Y. Tachibana, T. Shikada, *J. Catal.*, **1995**, *151*, 323-329. [Crossref], [Google Scholar], [Publisher]
20. K.P. Tikhomolova, I.B. Dmitrieva, M.V. Ivanova, *Russ. J. Appl. Chem.*, **1998**, *4*, 550-555. [Elibrary], [Google Scholar], [Publisher]
21. G.R. Dube, V.S. Darshane, *Bull. Chem. Soc. Jpn.*, **1991**, *64*, 2449-2453. [Crossref], [Google Scholar], [Publisher]
22. N.M. Deraz, *J. Anal. Appl. Pyrolysis*, **2008**, *82*, 212-222. [Crossref], [Google Scholar], [Publisher]
23. F.C. Romeijn, *Philips Res. Rep.*, **1953**, *8*, 304. [Crossref], [Google Scholar], [Publisher]
24. G. Blasse, *Philips Res. Rep. Suppl.*, **1964**, *3*, 96. [Crossref], [Google Scholar], [Publisher]
25. R. Parella, A. Kumar, S. Arulananda Babu, *Tetrahedron Lett.*, **2013**, *54*, 1738-1742. [Crossref], [Google Scholar], [Publisher]
26. A.R. Hajipour, M. Karimzadeh, G. Azizi, *Chin. Chem. Lett.*, **2014**, *25*, 1382-1386. [Crossref], [Google Scholar], [Publisher]
27. G. Satish, K.H. Vardhan Reddy, B.S.P. Anil, J. Shankar, R.U. Kumar, Y.V.D. Nageswar, *Tetrahedron Lett.*, **2014**, *55*, 5533-5538. [Crossref], [Google Scholar], [Publisher]
28. T. Liu, L. Wang, P. Yang, B. Hu, *Mater. Lett.*, **2008**, *62*, 4056-4058. [Crossref], [Google Scholar], [Publisher]
29. Z. Sun, L. Liu, D. Z. Jia, W. Pan, *Sens. Actuators B*, **2007**, *125*, 144-148. [Crossref], [Google Scholar], [Publisher]
30. D. Yang, B. An, W. Wei, M. Jiang, J. You, H. Wang, *Tetrahedron Lett.*, **2014**, *70*, 3630-3634. [Crossref], [Google Scholar], [Publisher]
31. G. Satish, K.H. Vardhan Reddy, K. Ramesh, B.S.P. Anil Kumar, Y.V.D. Nageswar, *Tetrahedron Lett.*, **2014**, *55*, 2596-2599. [Crossref], [Google Scholar], [Publisher]
32. R.K. Akula, C.S. Adimulam, S. Gangaram, R. Kengiri, N. Banda, *Lett. Org. Chem.*, **2014**, *11*, 440-445. [Crossref], [Google Scholar], [Publisher]
33. B.S.P. Anil Kumar, K.H. Vardhan Reddy, B. Madhav, K. Ramesh, Y.V.D. Nageswar, *Tetrahedron Lett.*, **2012**, *53*, 4595-4599. [Crossref], [Google Scholar], [Publisher]
34. B. Sreedhar, A. Suresh Kumar, D. Yada, *Tetrahedron Lett.*, **2011**, *52*, 3565-3569. [Crossref], [Google Scholar], [Publisher]
35. K.L. Chandra, P. Saravanan, R.K. Singh, V.K. Singh, *Tetrahedron*, **2002**, *58*, 1369-1374. [Crossref], [Google Scholar], [Publisher]
36. S. Kanta De, *Tetrahedron Lett.*, **2004**, *45*, 2919-2922. [Crossref], [Google Scholar], [Publisher]
37. A.K. Chakraborti, L. Sharma, R. Gulhane, Shivani, *Tetrahedron*, **2003**, *59*, 7661-7668. [Crossref], [Google Scholar], [Publisher]
38. A.K. Chakraborti, R. Gulhane, *Chem. Commun.*, **2003**, 1896-1897. [Crossref], [Google Scholar], [Publisher]
39. K. Jeyakumar, D. Kumar Chand, *J. Mol. Catal. A Chem.*, **2006**, *255*, 275-282. [Crossref], [Google Scholar], [Publisher]
40. Shivani, R. Gulhane, A.K. Chakraborti, *J. Mol. Catal. A Chem.*, **2007**, *264*, 208-213. [Crossref], [Google Scholar], [Publisher]

41. A.K. Chakraborti, R. Gulhane, *Tetrahedron Lett.*, **2003**, *44*, 3521-3525. **[Crossref], [Google Scholar], [Publisher]**
42. K.J. Ratnam, R.S. Reddy, N.S. Sekhar, M.L. Kantam, F. Figueras, *J. Mol. Catal. A Chem.*, **2007**, *276*, 230-234. **[Crossref], [Google Scholar], [Publisher]**
43. R. Alleti, M. Perambuduru, S. Samantha, V. Prakash Reddy, *J. Mol. Catal. A Chem.*, **2005**, *226*, 57-59. **[Crossref], [Google Scholar], [Publisher]**
44. R. Qiu, Y. Zhu, X. Xu, Y. Li, L. Shao, X. Ren, X. Cai, D. An, S. Yin, *Catal. Commun.*, **2009**, *10*, 1889-1892. **[Crossref], [Google Scholar], [Publisher]**
45. P. Christian, P. O'Brien, *J. Mater. Chem.*, **2005**, *15*, 4949-4954. **[Crossref], [Google Scholar], [Publisher]**

Copyright © 2021 by SPC (Sami Publishing Company) + is an open access article distributed under the Creative Commons Attribution License (CC BY) license (https://creativecommons.org/licenses/by/4.0/), which permits unrestricted use, distribution, and reproduction in any medium, provided the original work is properly cited.